Dynamic control of coherent pulses via Fano-type interference in asymmetric double quantum wells

Jin-Hui Wu,[1,2,*] Jin-Yue Gao,[1,2,†] Ji-Hua Xu,[3] L. Silvestri,[3] M. Artoni,[4,‡] G. C. La Rocca,[3,§] and F. Bassani[3]
[1]*College of Physics, Jilin University, Changchun 130023, People's Republic of China*
[2]*Key Laboratory of Coherent Light and Atomic and Molecular Spectroscopy of Ministry of Education, Changchun 130023, People's Republic of China*
[3]*Scuola Normale Superiore and INFM, Piazza dei Cavalieri 7, 56126 Pisa, Italy*
[4]*Department of Physics and Chemistry of Materials, Brescia University and LENS, Via Valotti 9, 25133 Brescia, Italy*
(Received 3 August 2005; published 19 May 2006)

We study the temporal and spatial dynamics of two light pulses, a probe and a switch, propagating through an asymmetric double quantum well where tunneling-induced quantum interference may be observed. When such an interference takes place, in the absence of the switch, the quantum well is transparent to the probe which propagates over sufficiently long distances at very small group velocities. In the presence of a relatively strong switch, however, the probe pulse is absorbed due to the quenching of tunneling-induced quantum interference. The probe may be made to vanish even when switch and probe are somewhat delayed with respect to one another. Conversely, our asymmetric double quantum well may be rendered either opaque or transparent to the switch pulse. Such a probe-switch "reciprocity" can be used to devise a versatile all-optical quantum interference-based solid-state switch for optical communication devices.

DOI: 10.1103/PhysRevA.73.053818 PACS number(s): 42.50.Gy, 78.67.De, 78.66.Fd, 42.50.Hz

I. INTRODUCTION

In the effort to reduce the size of today's microelectronics devices well below the micrometer range, different types of quantum effects highlighting the wave nature of electrons have become more and more appreciable. In double quantum well heterostructures, e.g., not only does one deal with quantum confinement of the electron wave function in quantum wells but also with tunneling of the electron wave function through the thin barriers of the wells [1,2]. In particular, quantum tunneling to a continuum from two resonant subband levels in asymmetric double quantum wells [3,4] may give rise to Fano-type interference which can be exploited, e.g., to devise a novel all-optical switching mechanism [5–8]. Although within a different context, it is worth mentioning here the importance that a continuum of states such as, e.g., autoionizing states [9,10] plays in controlling absorption via quantum interference effects in atomic media [11,12].

On the other hand, quantum optical phenomena in which the dynamics of a reference *probe* pulse can be efficiently controlled in time by a secondary light pulse have been the focus of several recent studies. Although a variety of such phenomena has been investigated in the past three decades and within different fields of physics, there is a renewed interest in such time-dependent propagation effects which may include simulton propagation [13], Raman solitons [14], enhanced nonlinear parametric generation [15,16], creation of matched pulses [17–19], and multiwave mixing processes in the ultraslow propagation regime [20,21], to mention a few. The latter are expected to have a wide range of applications in high-efficiency generation of short-wavelength, low-light intensity and single-photon nonlinear optics.

Time-dependent coherent control of the optical response of certain media that exhibit electromagnetic induced transparency [22,23] has also triggered a flurry of interest mainly for potential applications in the field of quantum information [24]. In such media, the presence of a *control* light pulse can make the group velocity v_g of a reference probe pulse to be either much slower [25] or faster [26] than the vacuum speed of light c, and in this case without contradicting causality. The probe may even be brought to a complete stop through a proper tailoring in time of the control pulse envelope. Experimental work to demonstrate some of these effects has been carried out in atomic gases [27–29] as well as in solid materials [30–33] which are certainly much better suited for applications.

In this paper we examine the time-dependent coherent control of light waves propagating in semiconductor heterostructures that exhibit Fano-type interference between adjacent intersubband transitions. This is a rather relevant issue which has remained so far unexplored, as far as we know, both theoretically and experimentally. A few authors have discussed the topic of coherent control of intersubband transitions in quantum wells [34–37], but they mainly focused on the absorption spectra and relaxation dynamics in three-level models while no propagation dynamics of coherent light pulses was considered. In Refs. [38–40], pulse propagation dynamics was considered and examined for a single exciton transition in a multiple-quantum-well Bragg structure, which again is different from our four-level quantum-well model for intersubband transitions. Our work also differs from the steady-state treatment of similar theoretical models studied, e.g., in [3,4,8], and which inherently miss

*Corresponding author. Email address: wujinhui0431@sina.com
†Email address: jygao@mail.jlu.edu.cn
‡Email address: artoni@lens.unifi.it
§Email address: larocca@sns.it

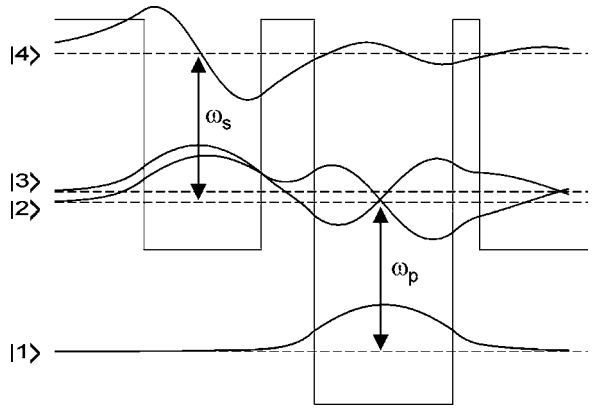

FIG. 1. Single period of the asymmetric quantum-well structure and relevant conduction subbands. The probe pulse with central frequency ω_p interacts with subband transitions $|1\rangle \leftrightarrow |2\rangle$ and $|1\rangle \leftrightarrow |3\rangle$, while the switch pulse with central frequency ω_s acts on subband transitions $|2\rangle \leftrightarrow |4\rangle$ and $|3\rangle \leftrightarrow |4\rangle$. Electrons in subband levels $|2\rangle$ and $|3\rangle$ decay to the same continuum by tunneling through the right thin barrier, leading to the Fano-type destructive interference. The solid curves represent the corresponding electron wave functions.

any time-dependent propagation dynamics. We will show that the latter becomes particularly rich in an asymmetric quantum well when two short laser pulses are tuned close to subband levels that decay to the same continuum.

Specifically, we examine the temporal and spatial dynamics of two coherent laser pulses, a probe and a switch, propagating through an asymmetric double quantum well designed so as to allow for a Fano-type interference to take place (see Fig. 1). By solving coupled Maxwell-Schrödinger equations as in Refs. [3,4,8,41–43], we find that in the absence of the switch, the probe pulse acting as a "signal" can propagate, with partial transparency due to the tunneling-induced quantum interference, and with a group velocity v_g much smaller than c. However, when the switch pulse is present tunneling-induced quantum interference is quenched and for switches stronger than the probe the latter will be almost completely absorbed over fairly short propagation lengths. This works as an absorptive optical switch [5] where a signal (probe) is fully controlled by another field (switch). Interestingly enough, this will occur even when the switch pulse lags slightly behind the probe which will be increasingly attenuated. Conversely, for probes stronger than the switch, the latter may be near-completely attenuated playing then itself the role of a signal, which would make the optical switch clearly more versatile.

II. THE MODEL

The asymmetric double quantum well with the relevant conduction band energy levels and wave functions is shown in Fig. 1. Two closely spaced delocalized intermediate levels $|2\rangle$ and $|3\rangle$ separated by the splitting 2Δ lay in between the ground-state level $|1\rangle$ (*deep well*) and the excited state level $|4\rangle$ (*shallow well*). A coherent pulse (probe) with central frequency ω_p couples the ground level $|1\rangle$ to the intermediate levels $|2\rangle$ and $|3\rangle$, while another coherent pulse (switch) with central frequency ω_s couples the upper level $|4\rangle$ with the two intermediate levels right below [44].

In the local (retarded) frame where $\tau = t - z/c$ and $\xi = z$, the propagation of the two pulses across the quantum well is described by the coupled Maxwell-Schrödinger equations,

$$\frac{\partial a_1}{\partial \tau} = j\Omega_p(\xi,\tau)(a_2 - a_3),$$

$$\frac{\partial a_2}{\partial \tau} = j\Omega_s(\xi,\tau)a_4 + j\Omega_p^*(\xi,\tau)a_1 + j[(\Delta_p + \Delta) + j\gamma_2]a_2 + \gamma_{23}a_3,$$

$$\frac{\partial a_3}{\partial \tau} = j\Omega_s(\xi,\tau)a_4 - j\Omega_p^*(\xi,\tau)a_1 + j[(\Delta_p - \Delta) + j\gamma_3]a_3 + \gamma_{23}a_2,$$

$$\frac{\partial a_4}{\partial \tau} = j\Omega_s^*(\xi,\tau)(a_2 + a_3) + j[(\Delta_p + \Delta_s) + j\gamma_4]a_4. \quad (1)$$

$$\frac{\partial \Omega_p(\xi,\tau)}{\partial \xi} = -j\frac{Nd_{12}^2\omega_p}{4\varepsilon_0 c\hbar}(a_1 a_2^* - a_1 a_3^*),$$

$$\frac{\partial \Omega_s(\xi,\tau)}{\partial \xi} = -j\frac{Nd_{24}^2\omega_s}{4\varepsilon_0 c\hbar}(a_2 a_4^* + a_3 a_4^*), \quad (2)$$

where $\Delta_p = \omega_p - (\omega_{21} + \omega_{31})/2$ and $\Delta_s = \omega_s - (\omega_{42} + \omega_{43})/2$ denote the probe and switch detunings, d_{ij} denotes the dipole moment of the $|i\rangle \leftrightarrow |j\rangle$ transition, and N is the electron density. As in the experiments [3,4,36,37], we consider transverse magnetic (TM) polarized pulses incident at an angle of 45 deg with respect to the growth axis so that all transition dipole moments include a factor $1/\sqrt{2}$ as intersubband transitions are polarized along the growth axis. Electrons in subband levels $|2\rangle$ and $|3\rangle$ rapidly decay, respectively, with rates $2\gamma_{2l}$ and $2\gamma_{3l}$, to the same continuum by tunneling through the thin barrier adjacent to the deep well. This gives rise to a Fano-type destructive quantum interference described by the cross-coupling term $\gamma_{23} = \sqrt{\gamma_{2l}\gamma_{3l}}$ between the two intermediate levels amplitudes a_2 and a_3 in Eqs. (1) [3]. In quantum wells, the overall relaxation rate γ_i of subband $|i\rangle$ comprises also a dephasing contribution γ_{id} so that the overall decay rate becomes $\gamma_i = \gamma_{il} + \gamma_{id}$. The latter contribution originates not only from electron-electron scattering and electron-phonon scattering, but also from inhomogeneous broadening due to interface roughness scattering. In high-quality samples at temperatures below 10 K and moderate doping levels γ_{id} may however be kept much smaller than γ_{il}.

The two pulses' space-time-dependent Rabi frequencies,

$$\Omega_p(\xi,\tau) = \frac{E_p^0 d_{12}}{\hbar} f(\xi,\tau) \equiv \Omega_p^0 f(\xi,\tau),$$

$$\Omega_s(\xi,\tau) = \frac{E_s^0 d_{24}}{\hbar} g(\xi,\tau) \equiv \Omega_s^0 g(\xi,\tau), \quad (3)$$

are here written in terms of the peak Rabi frequencies $(\Omega_{p,s}^0)$ and the dimensionless probe and switch pulse envelopes

$f(\xi,\tau)$ and $g(\xi,\tau)$ with durations τ_p and τ_s, respectively. We can further rewrite Eqs. (2)

$$\frac{\partial f(\xi,\tau)}{\partial \alpha\xi} = -j\frac{\gamma_2}{4\Omega_p^0}(a_1 a_2^* - a_1 a_3^*),$$

$$\frac{\partial g(\xi,\tau)}{\partial \beta\xi} = -j\frac{\gamma_4}{4\Omega_s^0}(a_2 a_4^* + a_3 a_4^*), \tag{4}$$

in terms of the two propagation constants

$$\alpha = \frac{Nd_{12}^2\omega_p}{\varepsilon_0 c\hbar\gamma_2}, \quad \beta = \frac{Nd_{24}^2\omega_s}{\varepsilon_0 c\hbar\gamma_4},$$

where α and β denote the probe and switch peak absorption coefficients [45]. We will restrict ourselves in the following to pulses with a "sin" waveform envelopes [46].

III. RESULTS AND DISCUSSION

In this section, we consider the case in which the barrier between the quantum wells is thin and levels $|2\rangle$ and $|3\rangle$ are almost equally delocalized over the two wells. We may then assume that $d_{12} \simeq -d_{13}$ and $d_{24} \simeq d_{34}$ for the choice of phase for the wave functions shown in Fig. 1. When γ_{2l} and γ_{3l} contribute to the overall rates γ_2 and γ_3 significantly more than γ_{2d} and γ_{3d} do, we can set $\gamma_{23} \simeq \gamma_2 \simeq \gamma_3$, in which case the double quantum well exhibits perfect tunneling-induced quantum interference. Realistic quantum-well structures, however, always have imperfect tunneling-induced quantum interference, i.e., $\gamma_{23} < \sqrt{\gamma_2\gamma_3}$, due to significant dephasing γ_{id}. Only with a proper design and preparation, the dephasing terms γ_{id} can be made small enough compared to the tunneling terms γ_{il} at very low temperatures [3,4], allowing then for near-perfect quantum interference. We here assume that all electrons are initially in the ground level $|1\rangle$, i.e., $|a_{11}(\tau=0)|^2=1$. Finally, for the sake of simplicity, we take $\alpha=\beta$, typical numerical values being $\alpha=\beta\simeq 10^4$ cm^{-1} [8]. Under these assumptions and with the realistic [3,4] quantum-well parameters used in Ref. [8], we solve numerically Eqs. (1) and (4).

We start by reporting in Fig. 2 the temporal and spatial evolutions of a probe pulse when the switch pulse is off. This is done for two different probe pulse durations, a parameter that turns out to be crucial in optimizing the propagation of the probe through the quantum well. We can see from Figs. 2(a) and 2(b) that in both cases the probe pulse can propagate with appreciable transparency even through a relatively long sample ($\xi=10/\alpha$ or $\xi=15/\alpha$) owing to high-quality tunneling-induced quantum interference. The probe, in fact, would be completely absorbed over lengths shorter than $\xi=10/\alpha$ if such a quantum interference does not exist or equivalently the two transitions $|1\rangle \leftrightarrow |3\rangle$ and $|2\rangle \leftrightarrow |3\rangle$ are irrelevant, which is indicated by Figs. 2(c) and 2(d). This extends to the pulsed regime results known already for plane waves [3,4], where control of interference between the two optical absorption paths of a cw probe in an asymmetric quantum-well structure was achieved by controlling the quantum tunneling from two resonant states of the well into

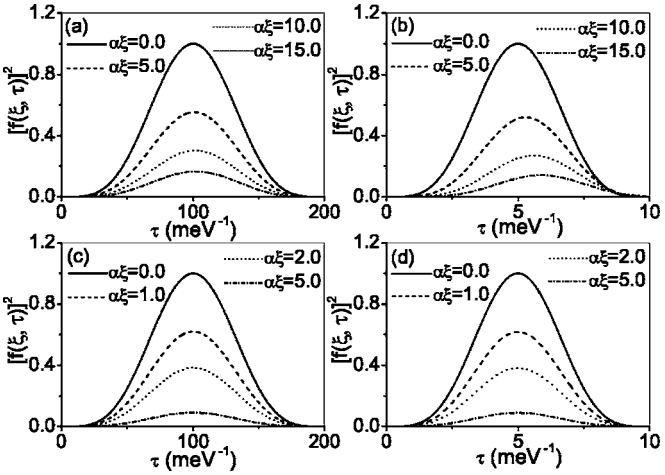

FIG. 2. Snapshots of the propagating probe pulse at different depths ξ of penetration into the sample in the absence of switch with (a) $\tau_p=200$ meV^{-1} and (b) $\tau_p=10$ meV^{-1}. The other parameters are $\gamma_{2l}=3.47$ meV, $\gamma_{2d}=0.68$ meV, $\gamma_{3l}=4.13$ meV, $\gamma_{3d}=0.80$ meV, $\Delta=4.36$ meV, $\Delta_p=0$, $\Omega_p^0=0.1$ meV, and $f(0,\tau)=\sin(\pi\tau/\tau_p)$. Parameters for (c) and (d), respectively, correspond to those for (a) and (b), but the cross-coupling terms γ_{23} in Eq. (1) have been removed in calculating the curves in (c) and (d).

the same energy continuum [47]. Here, the inverse of probe pulse duration τ_p is kept small enough with respect to various dephasing and decay rates so that substantial loss due to those far-off-resonant frequency components can be avoided.

The probe pulse group velocity at the frequency where the probe absorption is minimal can be approximately written [48] as

$$v_g = \frac{16\gamma_2\gamma_3\Delta^2}{\alpha(\gamma_2+\gamma_3)^3}, \tag{5}$$

which yields $v_g=8.3$ meV$/\alpha \simeq 0.042c$ for the realistic parameters $\gamma_2=4.15$ meV, $\gamma_3=4.93$ meV, and $\Delta=4.36$ meV. However, we find from Figs. 2(a) and 2(b) that $v_g=6.9$ meV$/\alpha$ for $\tau_p=200$ meV^{-1} and $v_g=17.0$ meV$/\alpha$ for $\tau_p=10$ meV^{-1}, which is somewhat different from the expected value [49]. The reason is that, as easily inferred from data in Ref. [8], the minimal probe absorption corresponds to $\Delta_p=-0.13$ meV rather than $\Delta_p=0$ as used here. Moreover, the probe pulse experiences a little more absorption when its duration becomes shorter, e.g., in a range from $\tau_p=200$ meV^{-1} to $\tau_p=10$ meV^{-1}.

One can quench the tunneling-induced quantum interference by a second field, making the quantum-well structure more opaque to the probe pulse, which may be used to devise a novel ultrafast and broadband optical switching mechanism [8]. Figure 3 shows the dynamical evolution of the probe pulse at different penetration lengths in the presence of the switch pulse. We have assumed that the probe and switch have the same profiles at the initial time, i.e., $f(0,\tau)=g(0,\tau)$. It is clear that, with a careful choice of the switch strength, one can attenuate the probe to a great extent when it goes through a sample of length of $\xi=8/\alpha$ or $\xi=15/\alpha$. From Figs. 3(a) and 3(b), we also see that the rela-

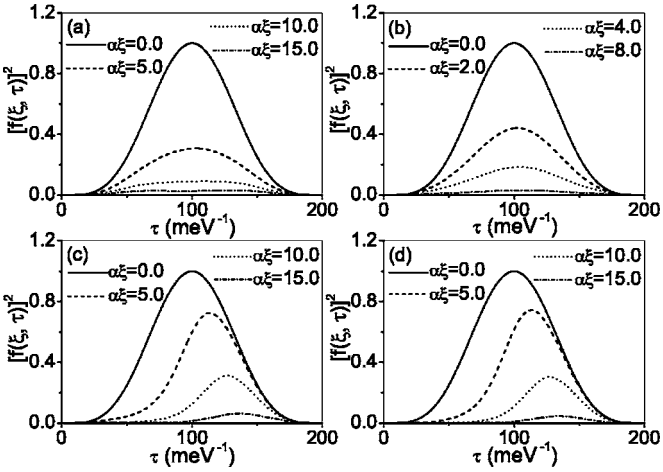

FIG. 3. Snapshots of the propagating probe pulse at different depths of penetration into the sample in the presence of the switch pulse with (a) $\Omega_p^0=0.1$ meV and $\Omega_s^0=1.0$ meV; (b) $\Omega_p^0=0.1$ meV and $\Omega_s^0=4.0$ meV; (c) $\Omega_p^0=0.4$ meV and $\Omega_s^0=4.0$ meV; (d) $\Omega_p^0=0.4$ meV and $\Omega_s^0=16.0$ meV. Other parameters are given as $\gamma_{2l}=3.47$ meV, $\gamma_{2d}=0.68$ meV, $\gamma_{3l}=4.13$ meV, $\gamma_{3d}=0.80$ meV, $\gamma_{4l}=0.80$ meV, $\gamma_{4d}=0.50$ meV, $\Delta=4.36$ meV, $\Delta_p=\Delta_s=0$, $\tau_p=\tau_s=200$ meV^{-1}, $f(0,\tau)=\sin(\pi\tau/\tau_p)$, and $g(0,\tau)=\sin(\pi\tau/\tau_s)$.

tively weak probe pulse is homogeneously and symmetrically absorbed. The reason is that almost all electrons remain in the ground level $|1\rangle$ all the times. However, for stronger probes their foregoing parts tend to be absorbed before their tails [see Figs. 3(c) and 3(d)]. This arises from the fact that for stronger probes the foregoing parts bleach the medium by pumping electrons, which will then decay to the continuum by tunneling into subbands $|2\rangle$ and $|3\rangle$. Consequently, one can not shorten the length at which the probe is near-completely absorbed just by increasing the switch pulse strength [see Figs. 3(c) and 3(d)]. It should be borne in mind that quenching of the tunneling-induced interference, or equivalently developing of the central absorption peak in Fig. 2(b) of Ref. [8], occurs for values of Ω_s^0 not much less than involved decay rates. This is because the dipole moment d_{01} of the central dressed transition $|0\rangle\leftrightarrow|1\rangle$ is proportional to $\Omega_s/\sqrt{2\Omega_s^2+\Delta^2}$, with Δ being of the order of γ_i, which directly follows from Eq. (7) in Ref. [8]. Moreover, in order to well attenuate the probe pulse, we should have $\tau_s \geqslant \tau_p$, which thus requires τ_s^{-1} being much smaller than various dephasing and decay rates.

It is worth noting that this mechanism is quite efficient. A probe with $\Omega_p^0=0.1$ meV can be near-completely attenuated by a ten times stronger switch with $\Omega_s^0=1.0$ meV and over a relatively short length ($\xi=15/\alpha$). Using a longer switch pulse ($\tau_s=2\tau_p$) one can show that the scheme can be made even more efficient by further reducing the residual energy at the wings of the probe pulse.

In Fig. 4, we consider the case of two pulses with the same profiles and separated by a short time delay $\Delta\tau$. The weak probe anticipates the strong switch so that the leading part of the probe propagates with a smaller group velocity than the switch following behind at a velocity of order of c. In a quantum well of length $\xi=15/\alpha$, the switch field will finally catch up with the probe, which will then tend to be

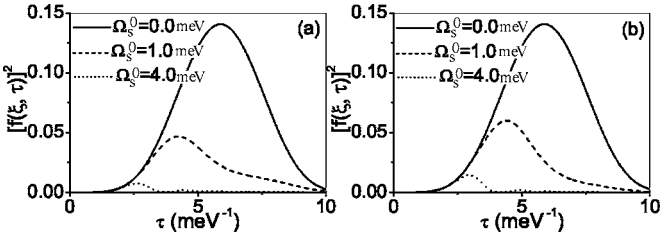

FIG. 4. Snapshots of the probe pulse propagating through a quantum well of length $\alpha\xi=15$ with (a) $g(0,\tau)=\sin[\pi(\tau-0.5\ \text{meV}^{-1})/\tau_s]$; (b) $g(0,\tau)=\sin[\pi(\tau-1.0\ \text{meV}^{-1})/\tau_s]$. Other parameters are the same as in Fig. 3(a) except $\tau_p=\tau_s=10$ meV^{-1}.

absorbed as long as the time delay is not too large and the switch not too weak. Unlike for the case of $\Delta\tau=0$, the probe pulse is first attenuated at its tail and then at its foregoing part. It is easy to understand that if the switch pulse slightly anticipates the probe, the quantum well will become transparent to the tail of the probe pulse while remaining absorbing to its foregoing part, which certainly results in much more flexible control of the probe pulse. In $GaAs/Al_xGa_{1-x}As$ or $In_xGa_{1-x}As/AlAs$, the inverse of the propagation constant α is of the order of 1 μm, and the distance of $\xi=15/\alpha$ over which the signal undergoes nearly complete absorption can be achieved using a sample with several periods inside an optical resonator in a multiple-pass configuration [50].

In Fig. 5, we consider the reverse case where a strong probe controls the propagation of a weak switch. The switch can be severely attenuated by the probe, which makes the switch behave as a signal and the probe as a "control" beam. Notice, however, that the physics governing the two cases of this peculiar "reciprocity" differs from one case to the other. Here, a signal in the "on" position, in fact, propagates with no loss owing to the lack of electrons in subbands $|2\rangle$ and $|3\rangle$,

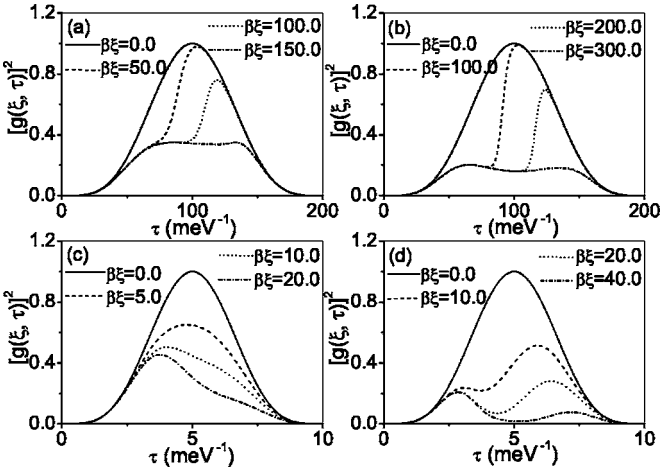

FIG. 5. Snapshots of the propagating switch pulse at different depths of penetration in the presence of the probe pulse with (a) $\Omega_p^0=2.0$ meV and $\tau_p=\tau_s=200.0$ meV^{-1}; (b) $\Omega_p^0=4.0$ meV and $\tau_p=\tau_s=200.0$ meV^{-1}; (c) $\Omega_p^0=2.0$ meV and $\tau_p=\tau_s=10.0$ meV^{-1}; (d) $\Omega_p^0=4.0$ meV and $\tau_p=\tau_s=10.0$ meV^{-1}. Other parameters are the same as in Fig. 3(a) except $\Omega_s^0=0.1$ meV.

while a signal in the "off" position is damped owing to the induced absorption process whereby one photon from each of the two beams is absorbed, exciting an electron from the ground state to level $|4\rangle$. Comparing Figs. 5(a) and 5(b) with 5(c) and 5(d), we also can see that a relatively shorter quantum well can be used to well eliminate the weak switch with a shorter duration because much less photons are involved in the propagation.

IV. CONCLUSIONS

In summary, we have investigated in detail the propagation dynamics of two coherent pulses, a probe and a switch, in a specific asymmetric double quantum well where tunneling-induced quantum interference may take place and be easily tuned. In the absence of one of the two pulses, tunneling-induced quantum interference is quite appreciable so that the other pulse can propagate with partial transparency at a reduced group velocity, or without loss at a group velocity of order of c due to the absence of electrons in certain subbands. Conversely, absorption and quenching of tunneling-induced quantum interference appearing when both pulses are present affect the propagation of one pulse, which may even undergo nearly complete attenuation. We have used numerical simulations and realistic quantum well parameters to investigate the two opposite situations in which either a strong switch can strongly attenuate a weaker probe or a strong probe attenuate a weaker switch. The specific quantum-well structure examined here may be exploited to devise an all-optical switching scheme where the two pulses can interchangeably play the roles of signal and control fields. Their reciprocity, in particular, would make a more versatile switch, enabling one to use distinct wavelengths for either signal or control which may turn out to be useful in designing quantum interference-based solid-state devices for optical communications.

ACKNOWLEDGMENTS

This work is supported by NSFC (Grants Nos. 10334010 and 10404009), MAE (Grant ST China-Italy), and MIUR (Accion Integrada Italia-Spagna IT1603). Jin-Hui Wu is grateful for the hospitality at the Scuola Normale Superiore in Pisa.

[1] E. H. Hauge and J. A. Stovneng, Rev. Mod. Phys. **61**, 917 (1989).
[2] R. Ferreira and G. Bastard, Rep. Prog. Phys. **60**, 345 (1997).
[3] H. Schmidt, K. L. Campman, A. C. Gossard, and A. Imamoglu, Appl. Phys. Lett. **70**, 3455 (1997).
[4] J. Faist, F. Capasso, C. Sirtori, K. West, and L. N. Pfeiffer, Nature (London) **390**, 589 (1997).
[5] S. E. Harris and Y. Yamamoto, Phys. Rev. Lett. **81**, 3611 (1998).
[6] X. M. Su and J. Y. Gao, Phys. Lett. A **264**, 346 (2000).
[7] M. Yan, E. G. Rickey, and Y. Zhu, Phys. Rev. A **64**, 041801(R) (2001).
[8] J. H. Wu, J. Y. Gao, J. H. Xu, L. Silvestri, M. Artoni, G. C. La Rocca, and F. Bassani, Phys. Rev. Lett. **95**, 057401 (2005).
[9] U. Fano, Phys. Rev. **124**, 1866 (1961); N. E. Karapanagioti, O. Faucher, Y. L. Shao, D. Charalambidis, H. Bachau, and E. Cormier, Phys. Rev. Lett. **74**, 2431 (1995). Artificial autoionizing states may also be generated leading to laser-induced continuum structures (LICS) originally studied by P. L. Knight, M. A. Lauder, and B. J. Dalton, Phys. Rep. **190**, 1 (1990); S. Cavalieri, F. S. Pavone, and M. Matera, Phys. Rev. Lett. **67**, 3673 (1991).
[10] More recent work on LICS may be found, e.g., in K. Bohmer, T. Halfmann, L. P. Yatsenko, D. Charalambidis, A. Horsmans, and K. Bergmann, Phys. Rev. A **66**, 013406 (2002).
[11] R. Eramo, S. Cavalieri, L. Fini, M. Matera, and L. F. DiMaurox, J. Phys. B **30**, 3789 (1997).
[12] O. Faucher, E. Hertz, B. Lavorel, R. Chaux, T. Dreier, H. Berger, and D. Charalambidis, J. Phys. B **32**, 4485 (1999).
[13] M. J. Konopnicki and J. H. Eberly, Phys. Rev. A **24**, 2567 (1981).
[14] J. R. Ackerhalt and P. W. Milonni, Phys. Rev. A **33**, 3185 (1986).
[15] S. H. Choi and G. Vemuri, Opt. Commun. **153**, 257 (1998).
[16] E. Paspalakis, N. J. Kylstra, and P. L. Knight, Phys. Rev. A **65**, 053808 (2002).
[17] S. E. Harris, Phys. Rev. Lett. **70**, 552 (1993).
[18] J. H. Eberly, A. Rahman, and R. Grobe, Phys. Rev. Lett. **76**, 3687 (1996).
[19] V. V. Koslov and J. H. Eberly, Opt. Commun. **179**, 85 (2000).
[20] H. Kang and Y. Zhu, Phys. Rev. Lett. **91**, 093601 (2003).
[21] M. G. Payne and L. Deng, Phys. Rev. A **65**, 063806 (2002).
[22] S. E. Harris, Phys. Today **50**(7), 36 (1997), and references therein.
[23] M. Fleischhauer, A. Imamoglu, and J. P. Marangos, Rev. Mod. Phys. **77**, 633 (2005).
[24] M. D. Lukin, Rev. Mod. Phys. **75**, 457 (2003).
[25] L. V. Hau, S. E. Harris, Z. Dutton, and C. H. Behroozi, Nature (London) **397**, 594 (1999).
[26] L. J. Wang, A. Kuzmich, and A. Dogarui, Nature (London) **406**, 277 (2000); X. -M. Hu, G. -L. Zou, X. Li, and D. Du, Phys. Rev. A **72**, 023803 (2005).
[27] M. Jain, H. Xia, G. Y. Yin, A. J. Merriam, and S. E. Harris, Phys. Rev. Lett. **77**, 4326 (1996).
[28] A. S. Zibrov, M. D. Lukin, and M. O. Scully, Phys. Rev. Lett. **83**, 4049 (1999).
[29] C. Liu, Z. Dutton, C. H. Behroozi, and L. V. Hau, Nature (London) **409**, 490 (2001).
[30] J. J. Longdell, E. Fraval, M. J. Sellars, and N. B. Manson, Phys. Rev. Lett. **95**, 063601 (2005).
[31] A. V. Turukhin, V. S. Sudarshanam, M. S. Shahriar, J. A. Musser, B. S. Ham, and P. R. Hemmer, Phys. Rev. Lett. **88**, 023602 (2002).
[32] P. R. Hemmer, A. V. Turukhin, M. S. Shahriar, and J. A. Musser, Opt. Lett. **26**, 361 (2001).
[33] B. S. Ham and P. R. Hemmer, Phys. Rev. Lett. **84**, 4080

(2000).
[34] X. Hu and W. Potz, Phys. Rev. Lett. **82**, 3116 (1999).
[35] W. Potz, Physica E (Amsterdam) **7**, 159 (2001).
[36] T. Muller, R. Bratschitsch, G. Strasser, and K. Unterrainer, Appl. Phys. Lett. **79**, 2755 (2001).
[37] T. Muller, W. Parz, G. Strasser, and K. Unterrainer, Phys. Rev. B **70**, 155324 (2004).
[38] N. C. Nielsen, S. Linden, J. Kuhl, J. Forstner, A. Knorr, S. W. Koch, and H. Giessen, Phys. Rev. B **64**, 245202 (2001).
[39] N. C. Nielsen, J. Kuhl, M. Schaarschmidt, J. Forstner, A. Knorr, S. W. Koch, G. Khitrova, H. M. Gibbs, and H. Giessen, Phys. Rev. B **70**, 075306 (2004).
[40] T. H. Z. Siederdissen, N. C. Nielsen, J. Kuhl, M. Schaarschmidt, J. Forstner, A. Knorr, G. Khitrova, H. M. Gibbs, S. W. Koch, and H. Giessen, Opt. Lett. **30**, 1384 (2005).
[41] G. B. Serapiglia, E. Paspalakis, C. Sirtori, K. L. Vodopyanov, and C. C. Phillips, Phys. Rev. Lett. **84**, 1019 (2000).
[42] T. Muller, W. Parz, G. Strasser, and K. Unterrainer, Appl. Phys. Lett. **84**, 64 (2004).
[43] C. R. Lee, Y. C. Li, F. K. Men, C. H. Pao, Y. C. Tsai, and J. F. Wang, Appl. Phys. Lett. **86**, 201112 (2005).
[44] Through a different design of the $Al_xGa_{1-x}As/GaAs$ quantum well shown in Fig. 1 the upper level may be moved below the two intermediate levels $|2\rangle$ and $|3\rangle$. In this case a properly modified version of this model could also describe a double-lambda configuration with a ground ($|1\rangle$) and a metastable ($|4\rangle$) state.
[45] Assuming as usual that the lower and upper levels of the relevant transitions are, respectively, occupied and empty.
[46] Similar results may be obtained using "Gaussian" or "sech" pulses.
[47] With no switch, in fact, our four-level double well reduces to the three-level configuration used in [3,4].
[48] E. Paspalakis, N. J. Kylstra, and P. L. Knight, Phys. Rev. Lett. **82**, 2079 (1999).
[49] Following a common usage in semiconductor physics, times are here given in units of the Planck constant $\hbar$ so that to the energy of 1 meV ($\hbar\nu=\hbar/\tau=10^{-3}$ eV) corresponds to a time $\tau=(\hbar)10^3\ \mathrm{eV}^{-1}\cong 4.1$ ps, which amounts in our case to pulse durations ranging between several tens and hundreds of picoseconds. Likewise for frequencies, the energy of 1 meV corresponds a frequency $\nu=10^{-3}\ \mathrm{eV}/(\hbar)=242$ GHz.
[50] D. Dini, R. Kohler, A. Tredicucci, G. Biasiol, and L. Sorba, Phys. Rev. Lett. **90**, 116401 (2003).